Electronic Supplementary Information for

Direct nanoimprinting of nanoporous organosilica films consisting of covalently crosslinked photofunctional frameworks

Norihiro Mizoshita,* Yuri Yamada, Masakazu Murase, Yasutomo Goto and Shinji Inagaki

Contents

1. NMR Spectra of Compounds 1 and 2

Compounds **1** and **2** were synthesized according to Scheme S1. The ^{1}H and ^{13}C NMR spectra of **1** and **2** are shown in Fig. S1 and S2, respectively.

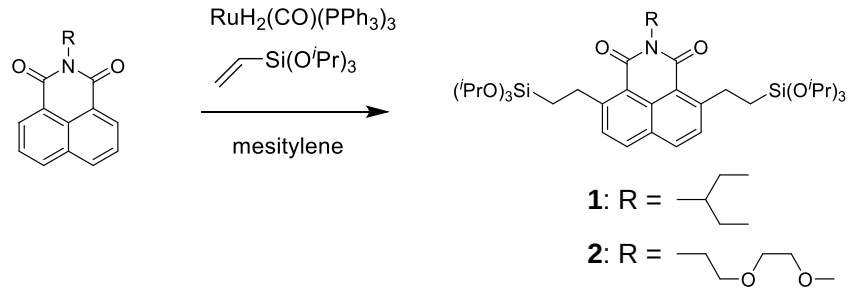

Scheme S1. Synthesis of organosilane precursors **1** and **2**.

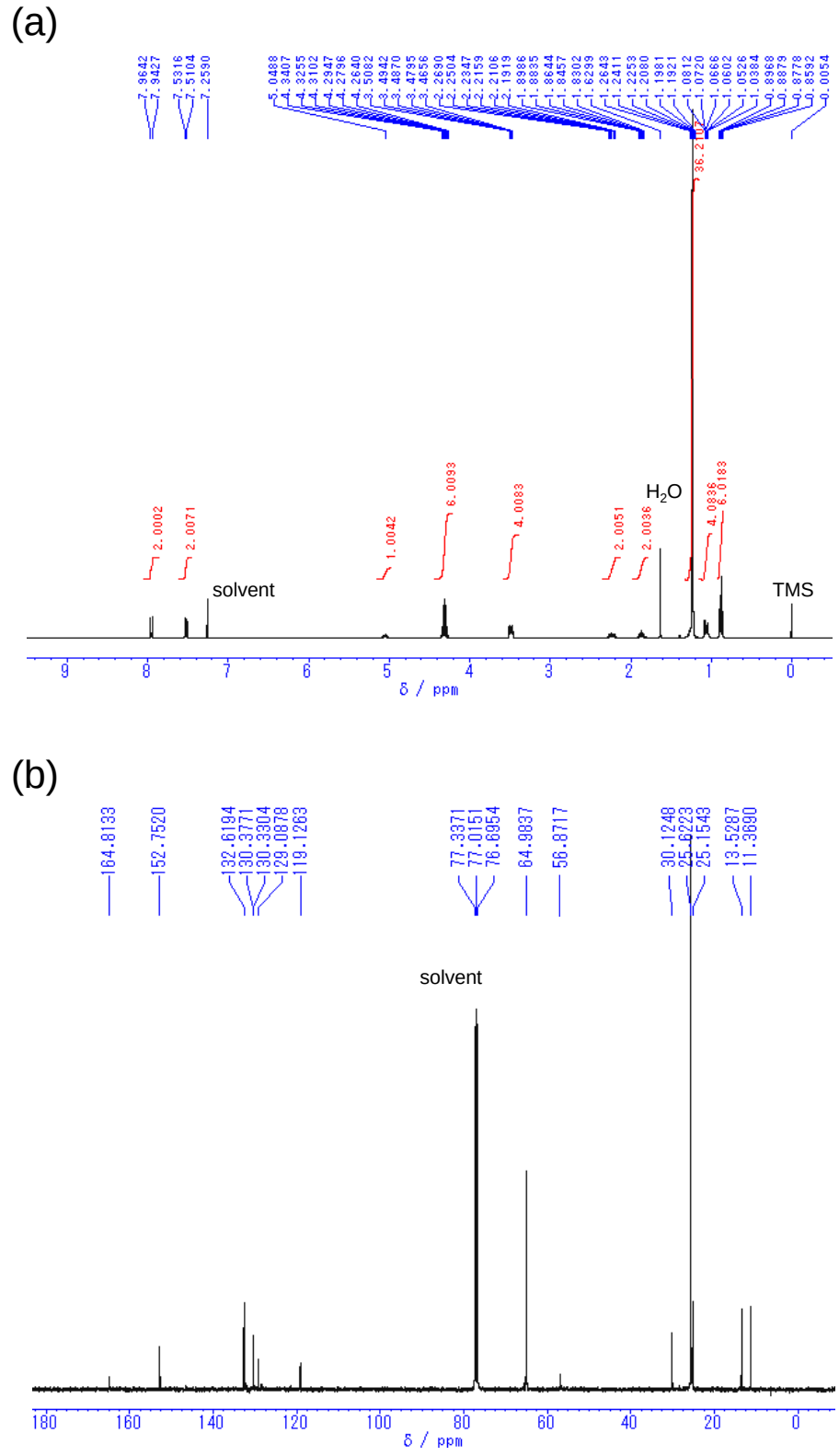

Fig. S1 (a) ^{1}H and (b) ^{13}C NMR spectra of **1** in $CDCl_3$.

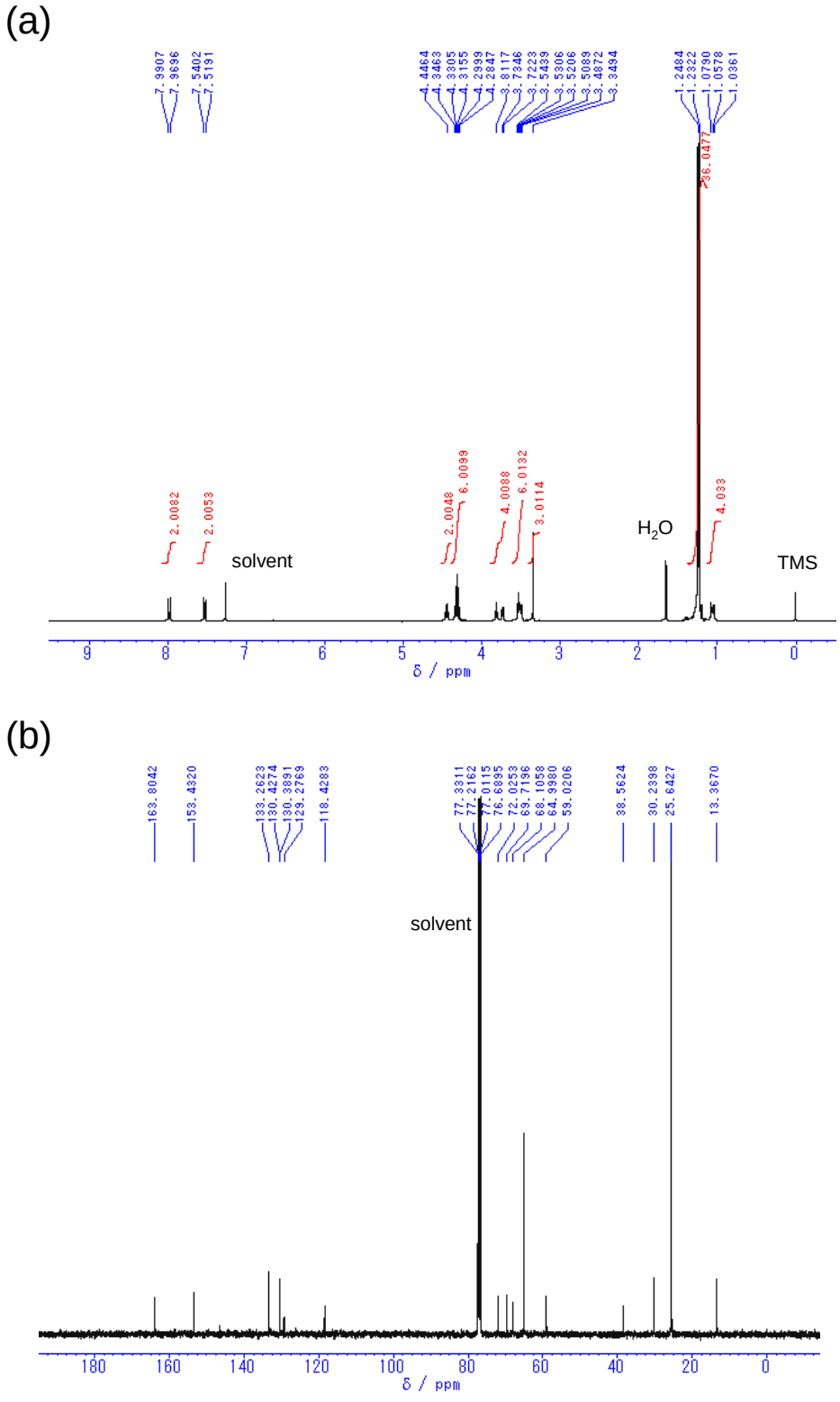

Fig. S2 (a) ^{1}H and (b) ^{13}C NMR spectra of **2** in $CDCl_3$.

2. Supplementary Data

2.1. UV-Vis Absorption Spectra

Fig. S3 shows UV-vis absorption spectra of **1**-silica and **2**-silica films prepared on a quartz substrate. These films have a strong absorption band around λ = 350 nm and can efficiently absorb the UV laser light used for LDI-MS (λ = 337 or 355 nm). The molar extinction coefficient of the naphthalimide group at λ = 337 nm is 1.3×10^4 M^{-1} cm^{-1} in CH_2Cl_2. The absorption coefficient of the organosilica films are determined to be $(7.6–8.0) \times 10^4$ cm^{-1} from the thickness and the absorbance.

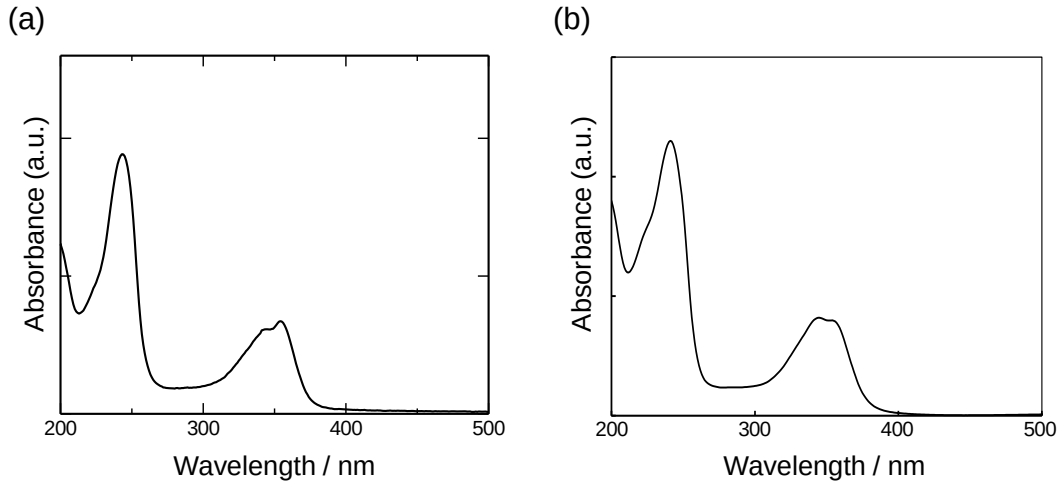

Fig. S3 UV-vis absorption spectra of (a) **1**-silica and (b) **2**-silica.

2.2. Large-Scale Nanoimprinting

Fig. S4 shows SEM images observed at different positions of a nanoimprinted **1**-silica film with a size of ca. 1.5×1.5 cm. Formation of vertically oriented nanoporous structures can be confirmed in most areas although partial distorted structure is seen in the edge region. This result indicates that homogeneous surface nanostructures can be formed on the organosilica films by a centimeter-scale nanoimprinting.

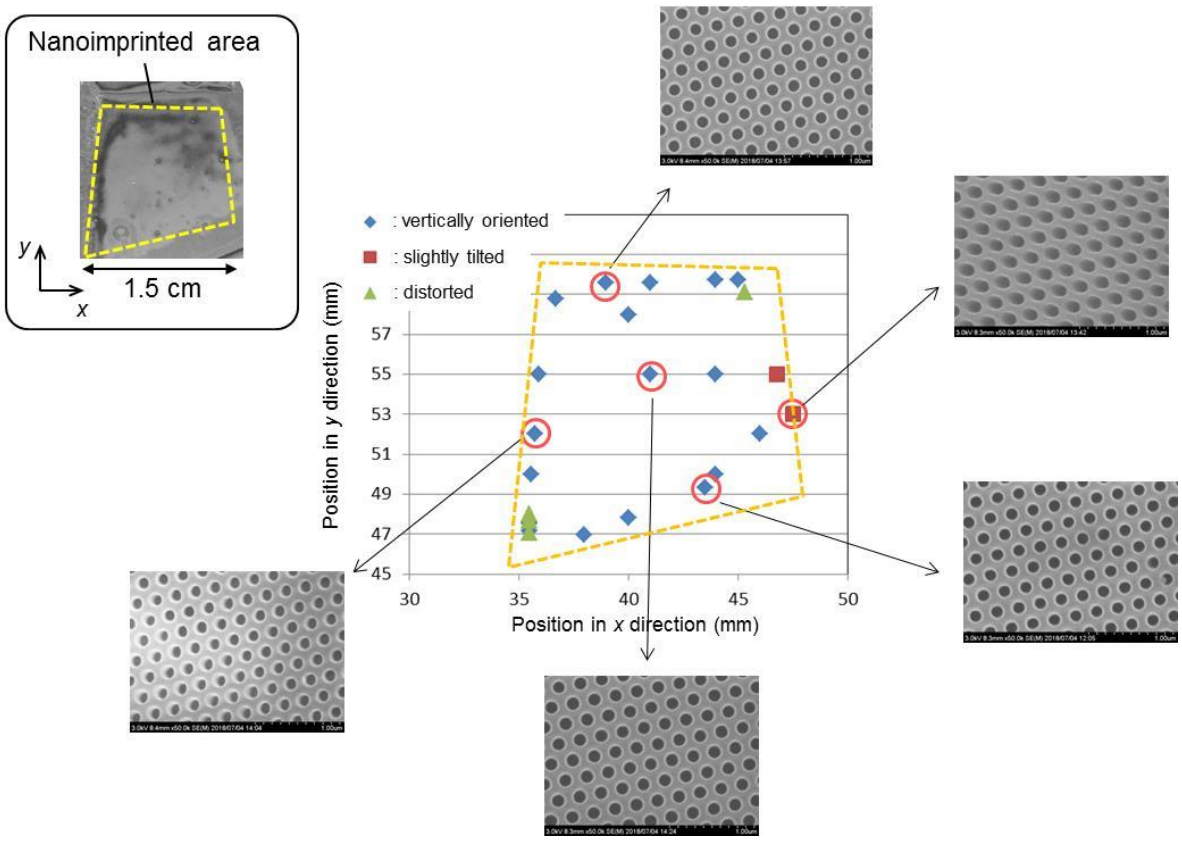

Fig. S4 SEM observation of the nanoporous structures in various positions on the nanoimprinted **1**-silica film.

2.3. Thermal Properties

Thermogravimetric analysis of the organosilicas was conducted on a Rigaku Thermo Plus TG 8120 under nitrogen atmosphere (Fig. S5). The temperature at which a 5% weight loss occurs was 370 °C for **1**-silica and 398 °C for **2**-silica. The slight weight loss is attributed to the dehydration due to the condensation of the residual silanols. No noticeable decomposition was observed up to at least 350 °C. The large weight loss due to the decomposition of organic groups occurred at 400–500 °C.

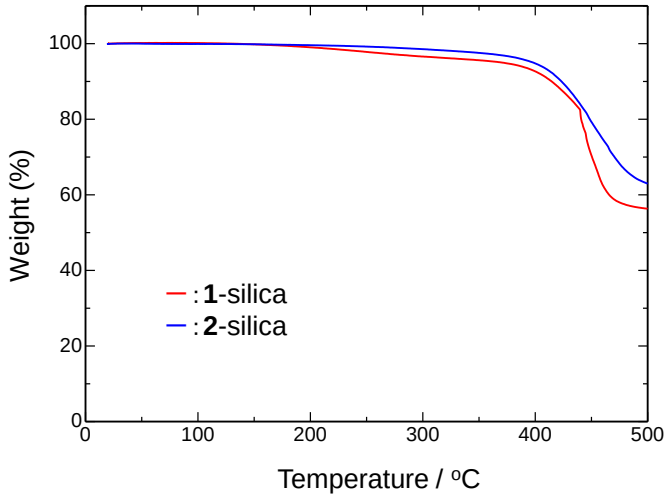

Fig. S5 Thermogravimetric analysis of **1**-silica and **2**-silica.

The thickness of the **1**-silica films was measured after various annealing treatments to evaluate the shrinkage in the direction of thickness. We used **1**-silica films with different initial thickness (343–395 nm). The films were annealed at 80–350 °C for 30 min, then the thickness was measured using an AFM. For each annealing treatment, thicknesses at different ten points were measured and averaged. Fig. S6 shows the relative thickness (%) of the annealed films to the initial films prepared at 25 °C. The thickness decreased with the increasing in the annealing temperature. The change due to thermal annealing is less than 1% within the range of conditions used for our nanoimprinting process (25–80 °C). Annealing at 220 °C reduced the thickness, but the change was less than 10% (5–8%). When the films were heated at 350 °C, the thickness was reduced by about 20%.

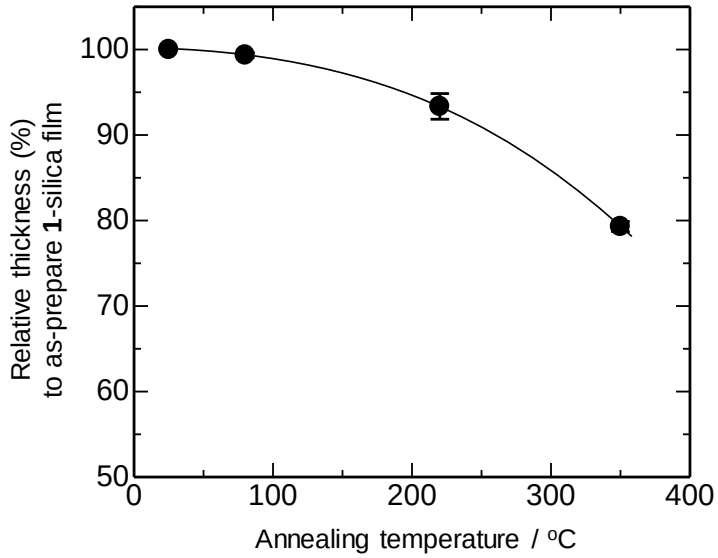

Fig. S6 Decrease in the thickness of **1**-silica films after annealing at 80–350 °C for 30 min.

Thermal conductivity (λ) of organosilica materials was calculated using the equation, $\lambda = \alpha c_p \rho$, where α is the thermal diffusivity, c_p is the heat capacity and ρ is the density of the material. Measurement of α was performed for 1mm-thick **1**-silica by a laser flash method using a Netzsch LFA 447 Nano Flash. The c_p was measured by differential scanning calorimetry using a Rigaku Thermo Plus DSC 8230. The ρ was measured on the basis of Archimedes' principle, using a Mettler Toledo Density Kit. The α, c_p, and ρ for **1**-silica were determined to be $(3.2 \pm 1.0) \times 10^{-7}$ m^2 s^{-1}, 1.50 J g^{-1} K^{-1}, and 1.12 g cm^{-3}, respectively, and the λ was calculated to be 0.54 ± 0.17 W m^{-1} K^{-1}.

2.4. Sol–Gel Reaction Control of 1

^{29}Si NMR spectra of a sol solution of **1** in 1-propanol are shown in Fig. 4. Here, classical notation T is used for the expression of the hydrolysis and condensation state of the trialkoxysilyl groups. T notation is completed by *i* and *j* indices (T^{ij}; *i*, *j* = 0, 1, 2 or 3), where *i* is the number of Si-O-Si bonds and *j* is the number of hydroxy functions. The assignment of the ^{29}Si NMR signals is given in Table S1. In the initial state of the solution, precursor **1** exhibited a single peak at –50.2 ppm corresponding to the triisopropoxysilyl groups (T^{00}). For reaction times of 0.25–1.0 h, T^0 species were mainly observed at –42.6 to –46.4 ppm, which indicates the smooth hydrolysis of the alkoxysilyl groups. In this stage, weak T^1 signals at –53.7 and –51.7 ppm were detected, suggesting only a partial condensation of the hydrolyzed precursors. For reaction times over 2.0 h, almost no T^0 species was detected and the T^1 signals were mainly observed. These results indicate that the main reaction shifts from hydrolysis to polycondensation at a reaction time of 1.0–2.0 h. The sol solutions reacted for more than 2.0 h mainly contain a polymeric species; therefore, the use of the well-reacted sol solutions leads to the excess hardening of the organosilica films immediately after the spin coating. Fig. S7a shows an AFM image of the nanoimprinted **1**-silica film prepared using a sol solution reacted for 5 h. Although a periodic pattern was observed on the surface, only distorted shallow hollows (depth: 30–40 nm) were formed for the film. This is because the nanopillar array on the surface of the polymer mold could not penetrate into the film due to the excess hardening of the organosilica film as shown in Fig. S7b.

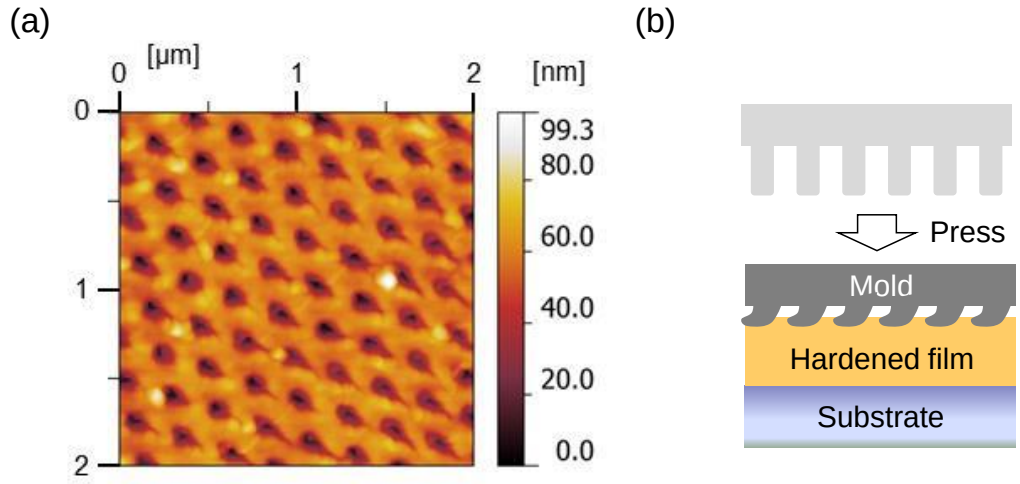

Fig. S7 (a) AFM image of a nanoimprinted **1**-silica film prepared using a sol solution after 5 h stirring. (b) Schematic illustration of the unsuccessful nanoimprinting process.

Table S1. Assignment of ^{29}Si NMR signals obtained for the sol solution of **1** in 1-propanol

Notation of Si species		Formula	Chemical shift (ppm)
T^i	T^{ij}		
T^0	T^{00}	R-***Si***(O^iPr)$_3$	−50.2
	T^{01}	R-(^{i}PrO)$_2$***Si***(OH)	−46.4
	T^{02}	R-(^{i}PrO)***Si***(OH)$_2$	−44.2
	T^{03}	R-***Si***(OH)$_3$	−42.6
T^1	T^{10}	R-(^{i}PrO)$_2$***Si***(OSi)	−53.7
	T^{11}	R-(^{i}PrO)***Si***(OSi)(OH)	−51.7
	T^{12}	R-***Si***(OSi)(OH)$_2$	−48.1[a]
T^2	T^{20}	R-(^{i}PrO)***Si***(OSi)$_2$	no data
	T^{21}	R-***Si***(OSi)$_2$(OH)	−57.8[a]
T^3	T^{30}	R-***Si***(OSi)$_3$	−67.0[a]

[a] Chemical shifts observed for **1**-silica powder obtained by hydrothermal treatment (100 ^{o}C, 20 h) using 28% aqueous NH_3 solution.

The hydrolyzed precursors with reactive silanols were converted into organosilica films on the substrate. The degrees of condensation were examined by solid-state ^{29}Si magic angle spinning (MAS) NMR measurements of the **1**-silica films annealed at 25 and 80 °C. Fig. S8 shows ^{29}Si MAS NMR spectra of the films. The NMR signals corresponding to T^n species (T^n: $-Si(OSi)_n(OH)_{3-n}$) were observed at –49.8 (T^1), –57.1 (T^2), and –67.2 (T^3) ppm. The degrees of condensations were calculated to be 64 and 66% for annealing temperatures of 25 and 80 °C, respectively. It should be noted that NMR signals attributed to residual –Si(O^{i}Pr) groups observed in the sol solutions (–52, –54, and –61 ppm) are not detected in the NMR spectra of the condensed films. We think that the evaporation of the organic solvent by spin coating concentrates the acid catalyst and promotes the hydrolysis of the alkoxysilyl group in the sol–gel films.

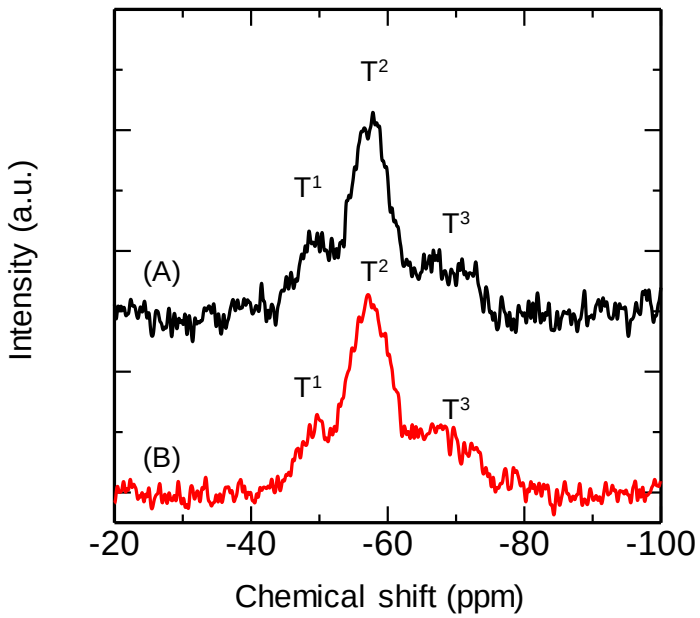

Fig. S8 ^{29}Si MAS NMR spectra of **1**-silica films annealed at (A) 25 and (B) 80 °C.

2.5. Nanoimprinting of a Fluorescent Organosilica Film

Fig. S9 shows a chemical structure of 1,6-diphenylpyrene (DPPy)-derived precursor DPPy-Si and an AFM image of the nanoimprinted DPPy-silica film. Nanoimprinting was performed for a DPPy-silica spin-coated film prepared using an acidic sol solution of DPPy-Si in 1,4-dioxane. The formation of a vertically oriented nanopore array was confirmed for the highly fluorescent organosilica film, which indicates the wide applicability of the nanoimprinting approach for organosilica materials.

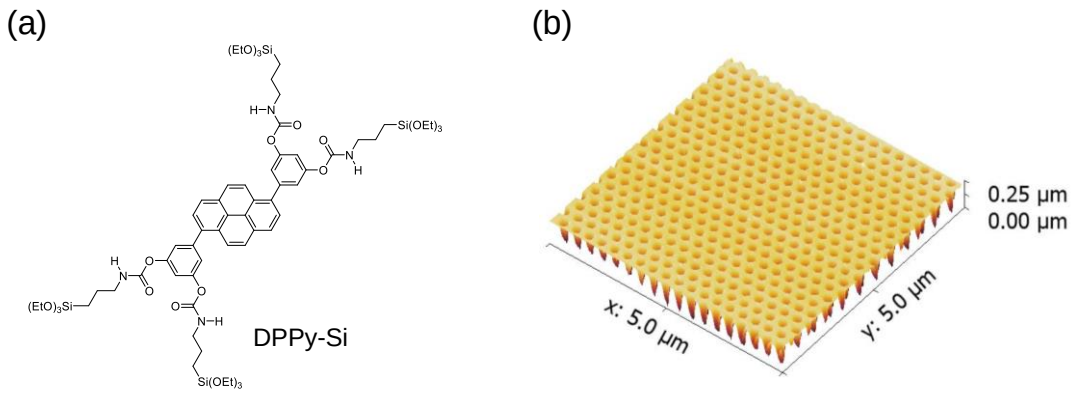

Fig. S9 (a) Molecular structure of DPPy-Si. (b) AFM image of a nanoimprinted DPPy-silica film.

2.6. Suppression of Low Molecular Weight Impurities

For the use of the organosilica films in LDI-MS, it is required that the organosilica framework itself shows almost no unnecessary peaks. To remove low molecular weight impurities and suppress the occurrence of noise from the organosilica framework, the as-deposited **1**-silica films were washed with ethanol (sonication, 30 min). Figure S10 shows LDI TOF mass spectra of A1 (m/z = 1296.7 for $[M+H]^+$) obtained by using the **1**-silica films before and after ethanol washing. For the as-deposited film, various low molecular weight species (m/z = 263–530) were strongly detected as shown in Fig. S10a. A peak at m/z = 263 is attributable to the ligand of a Ru complex used in the synthesis of **1** (triphenylphosphine, $[M+H]^+$). Most of these peaks disappeared after washing by sonication in ethanol (Fig. S10b).

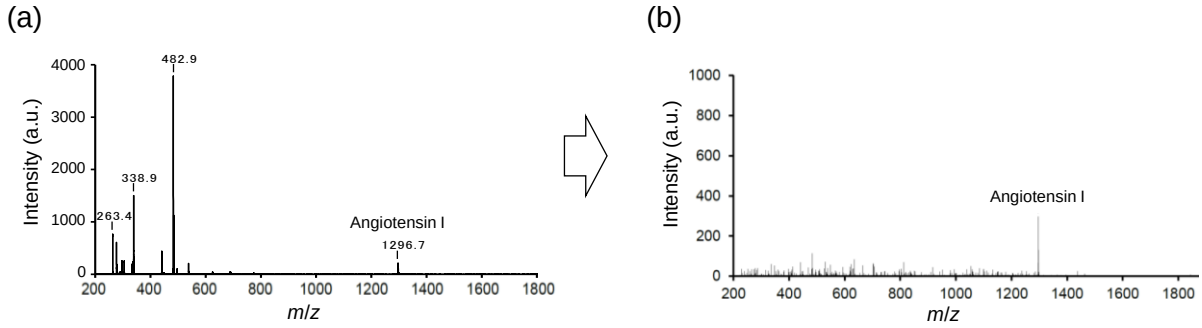

Fig. S10 LDI TOF mass spectra of A1 (1 pmol) measured using **1**-silica films: (a) as-deposited; (b) after washing by sonication in ethanol.

2.7. Supplementary Mass Spectra

Fig. S11a shows the LDI TOF mass spectrum of insulin obtained by the use of the nanoimprinted **1**-silica substrate. This result indicates that bio-related compounds with a molecular weight over 5000 can be desorbed and ionized by the present matrix-free LDI method. Fig. S11b shows the LDI TOF mass spectrum of A1 used for the determination of the limit of detection. The *S*/*N* ratio is ca. 3. When the loading amount of A1 was further decreased, no signal for A1 was detected.

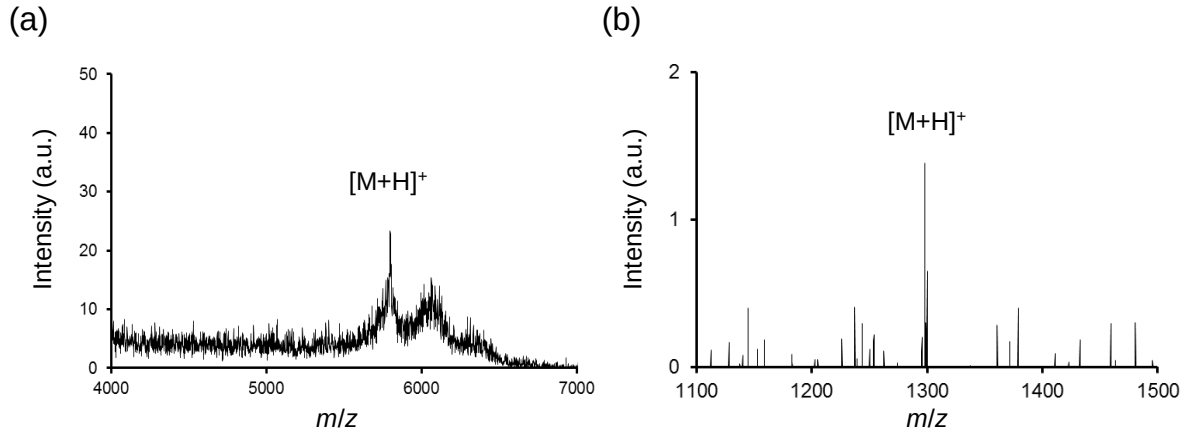

Fig. S11 LDI TOF mass spectrum of (a) insulin (5.0 pmol) and (b) A1 (75 fmol) obtained using the nanoimprinted **1**-silica substrate.

2.8. Formation of Hydrophobic Nanoparticle Layers

Fig. S12 shows SEM images of the spray-coated hydrophobic nanoparticle layers on the Si substrate. The nanoparticle aggregates form rough surface structures, which contributes to the induction of superhydrophobicity. It has been confirmed that the nanoparticle layers can endure the air blowing or solution flowing.

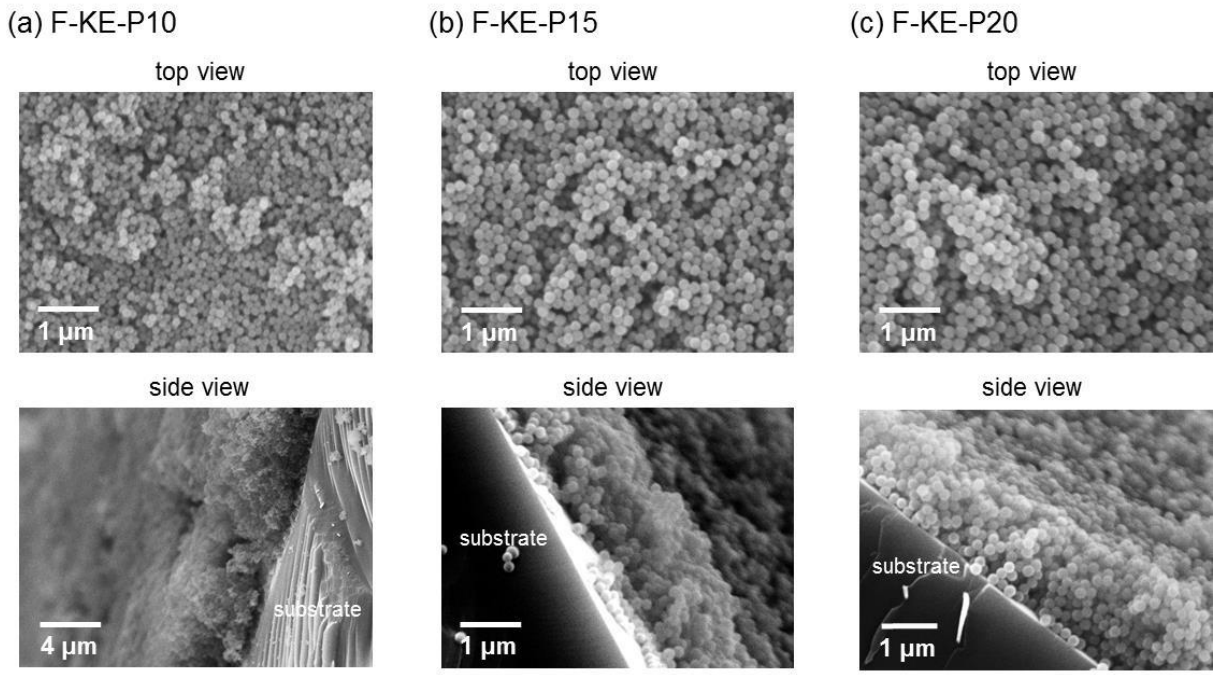

Fig. S12 SEM images of hydrophobic layers prepared on Si substrates by spray coating of silica nanoparticles modified with fluoroalkyl groups. Average diameter of nanoparticles: (a) 100 nm; (b) 150nm; (c) 200 nm.

Fig. S13a shows the procedure of the pattern formation by spray coating of the hydrophobic nanoparticles. All the spray-coated nanoparticle layers exhibit superhydrophobicity (Fig. S13b) and repel water droplets from the surface (Fig. S13c).

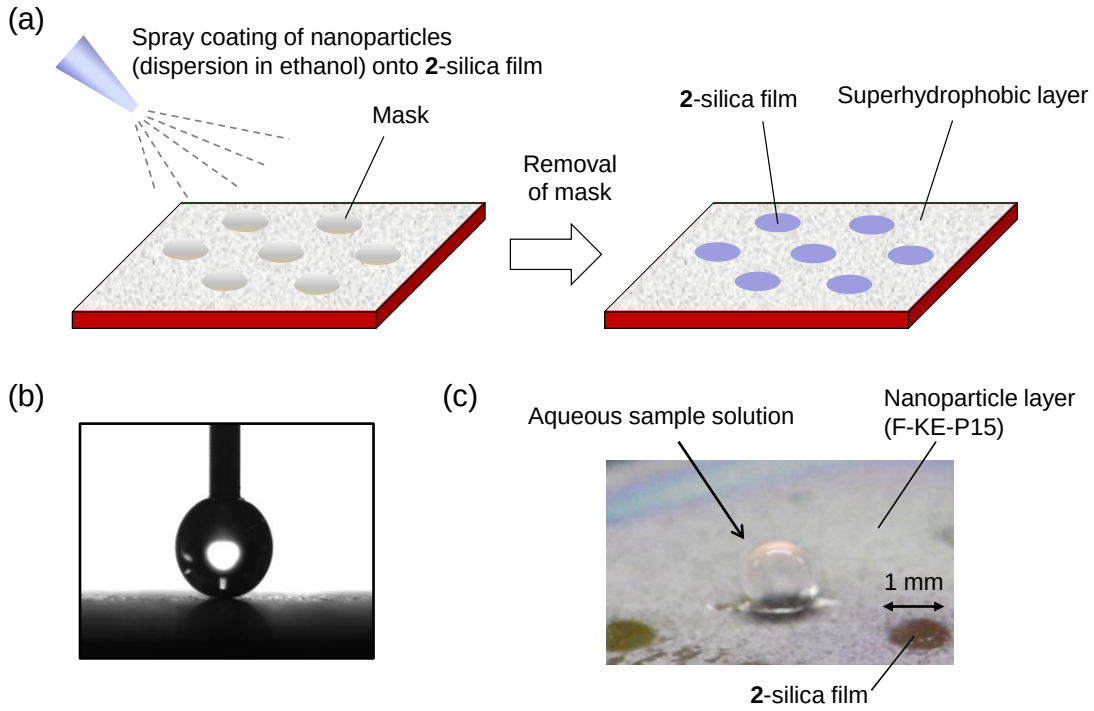

Fig. S13 (a) Preparation of a patterned hydrophobic layer by spray coating of a dispersion of hydrophobic nanoparticles. (b) Measurement of water contact angle for F-KE-P15 layer. (c) Photograph of the patterned substrate trapping a droplet of a sample solution.